Chandra OBSERVATIONS OF THE OPEN CLUSTER NGC 2516

F. R. Harnden, Jr.,[1] N. R. Adams,[1] F. Damiani,[2] J. J. Drake,[1] N. R. Evans,[1] F. Favata,[3] E. Flaccomio,[2] P. Freeman,[1] R. D. Jeffries,[4] V. Kashyap,[1] G. Micela,[2] B. M. Patten,[1] N. Pizzolato,[2] J. F. Schachter,[1,5] S. Sciortino,[2] J. Stauffer,[1] S. J. Wolk[1] and M. V. Zombeck[1]

ABSTRACT

Our analysis of *Chandra* X-ray Observatory data for the open cluster NGC 2516, sometimes referred to as "the southern Pleiades", has yielded over 150 X-ray detections in both HRC and ACIS images of the central region of the cluster. We identify some of the new X-ray sources with photometric cluster members and compare these new *Chandra* results with those of ROSAT. To date, 82 detected X-ray sources (42% of surveyed cluster members) are tentatively identified as cluster members. We also discuss the X-ray properties of late-type members in comparison with those of corresponding stellar types in the more metal rich approximately coeval Pleiades Cluster.

Subject headings: Open clusters and associations: NGC 2516 – Stars: coronae – X-rays: stars

1. Introduction

NGC 2516, at distance of a 387 pc (Jeffries, Thurston and Pye 1997; hereafter JTP97), can play an important role in the study of several fields of stellar physics: coronal activity, the relation of coronal activity to the temporal evolution of stellar structure, and the relation of stellar structure to metallicity. Based on ROSAT PSPC data, JTP97 have shown that the X-ray brightest dG members of NGC 2516 are less luminous than the brightest dG Pleiads. Since these two clusters are similar in age (both $\sim 10^8$yr), this makes NGC 2516 an exception to the established X-ray luminosity versus age correlation (JTP97). These same authors have tentatively linked this peculiarity to the measured low metallicity of its stars (NGC 2516 and the Pleiades have [Fe/H] = -0.32 and 0, respectively) and in particular to the effect of metallicity on the depth of the convective layer. According to the magnetic dynamo paradigm, it is the depth of the convective layer which affects rotational evolution, dynamo efficiency, and ultimately coronal activity at a given age in late-type stars (cf. also the discussion in Micela et al. 2000).

Previous studies of coronal emission were limited by the low sensitivity and spatial resolution of the instruments used, but thanks to the improved characteristic of the orbiting X-ray observatory *Chandra*, we can now establish with greater confidence the existence and extent of differences in X-ray luminosity and its dependence on stellar parameters. The present data, obtained as part of the calibration program at the start of the *Chandra* mission, allow us to reach a deeper limiting sensitivity with respect to previous studies, despite the shortness of these first exposures.

2. Data Analysis

2.1. X-ray data

Our data, whose characteristics are summarized in Table 1, comprise two observations of NGC 2516 with the ACIS-I (Advanced CCD Imaging Spectrometer - Imager; Townsley et al. 2000) and one

[1]Harvard-Smithsonian Center for Astrophysics, 60 Garden St. Cambridge, MA 02138

[2]Osservatorio Astronomico di Palermo G.S. Vaiana

[3]European Space Agency, Astrophysics Division

[4]Keele University

[5]Chase Securities

Table 1: Journal of NGC 2516 Observations

OBSID	Detector	Obs. date	exposure (ksec)
65	ACIS-I	1999-08-26	10.0
1232	ACIS-I	1999-08-27	9.6
1405	HRC-I	1999-10-25	20.4

Table 2: Observation and detection of identified NGC 2516 members vs. spectral type

Stars:	B	A	F	G	K	M
Observed	24	24	18	30	62	39
Detected	7	8	14	17	26	10

with the HRC-I (High Resolution Camera - Imager; Murray et al. 2000). The ACIS-I images, with their $16'$x$16'$ fields of view, were obtained one day apart with nearly identical pointing directions (RA = $7^{\rm h}$ $58^{\rm m}$ $20^{\rm s}$, Dec = -60° 47′ 33″). Because the latter of these two images experienced a strong, rapid increase in background level, we have first filtered out times of high background before properly registering and co-adding it with the first, in order to increase sensitivity.

The $30'$x$30'$ field-of-view HRC image was obtained with the telescope pointed at the position RA = $7^{\rm h}$ $57^{\rm m}$ $56^{\rm s}$, Dec = -60° 45′ 21″.

The HRC and ACIS images, shown at the same scale in Figs. 1 and 2, respectively, were analyzed using a wavelet-based source detection algorithm *pwdetect*, developed at the Osservatorio Astronomico di Palermo. The basic features of this code are inherited from a version developed for the analysis of ROSAT/PSPC data (Damiani et al. 1997a,b). Briefly, it performs a multi-scale analysis of the data, efficiently detecting sources ranging in size from point-like (~0.5 arcsec at image center) to a few arc minutes. The newest features of the *Chandra pwdetect* code include: operation on event lists (rather than binned images), full utilization of data information content on a wide range of spatial scales; and accurate evaluation of the non-gaussian transform statistics and background levels in the *Chandra* case of very low background (<< 1 cnt per resolution element – details will be presented by Damiani et al. in preparation). Large sets of simulations of pure-background HRC/ACIS images were performed in order to derive appropriate detection thresholds that limit spurious detections to the desired number (chosen here as 1 per field).

With this choice of thresholds, we find 160 sources from the ACIS-I image and an additional 9 HRC sources that were detected within the region covered by the ACIS field (12 other HRC sources found outside the ACIS field will be discussed in a forthcoming paper). Of the 160 ACIS sources, 13 were rejected as due to a "flaring pixel" instrumental effect[6], leaving a total of 156 detections (160-13+9) to be discussed below.

In order to derive source rates we have adopted the net source counts derived from *pwdetect* and individual source exposure times from properly computed exposure maps. For 89 of the brightest sources, we were also able to determine reliable ACIS-I hardness ratios (with "soft" and "hard" defined as 0.1–0.9 and 0.9–4.0 keV, respectively) and used these ratios to infer individual counts-to-flux conversion factors for these sources in the energy range from 0.1 to 4.0 keV. These values range from 7.6 to 11.9 $\times$ 10^{-12}erg cm^{-2}cnt^{-1}. For the remaining weaker sources, as well as for upper limits, we used a constant conversion factor of 9.07×10^{-12}erg cm^{-2} cnt^{-1} (inferred from the mean hardness ratio of the weaker sources). For sources detected only with the HRC-I, we used an estimated factor of 12.0×10^{-12}erg cm^{-2} cnt^{-1}, as determined with PIMMS using a single-temperature Raymond-Smith model with kT=0.5 keV and $N_H = 7.5\times10^{20}$ cm^{-2}, i.e., the mean N_H toward NGC 2516 derived from its mean reddening of E(B-V)= 0.12 (Cox 1995).

2.2. Cluster Membership and Identifications

An HR diagram of V vs. B-V is shown in Fig. 3 for photometrically determined members of NGC 2516. Photometry for stars brighter than V~9 comes from various sources (cf. JTP97), while photometry for the fainter stars is from a new catalogue (Jeffries, Thurston and Hambly, in preparation). Tentative cluster membership has been assigned by selecting stars within

[6] cf. http://asc.harvard.edu/udocs/acis/fi_pixels for a brief discussion

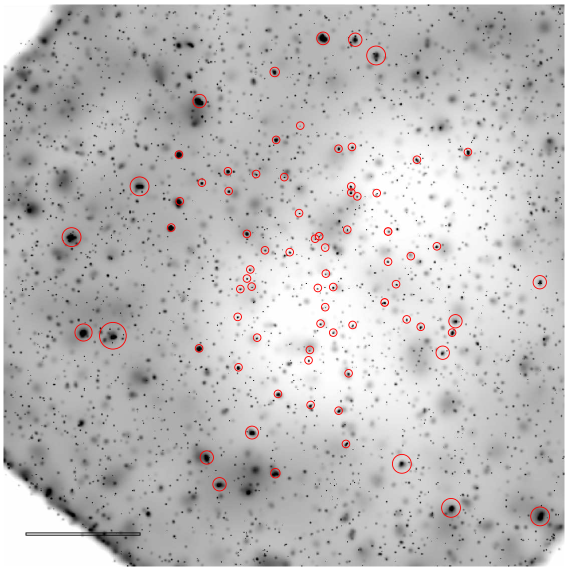

Fig. 1.— *Chandra* HRC-I data processed with the "CSMOOTH" adaptive smoothing algorithm of the CIAO package (*Chandra* Interactive Analysis of Observations - cf. http://asc.harvard.edu/ciao/). North is up and East, to the left. Circles indicate HRC-I detections, and image scale is indicated by a 5 arcmin bar at lower left.

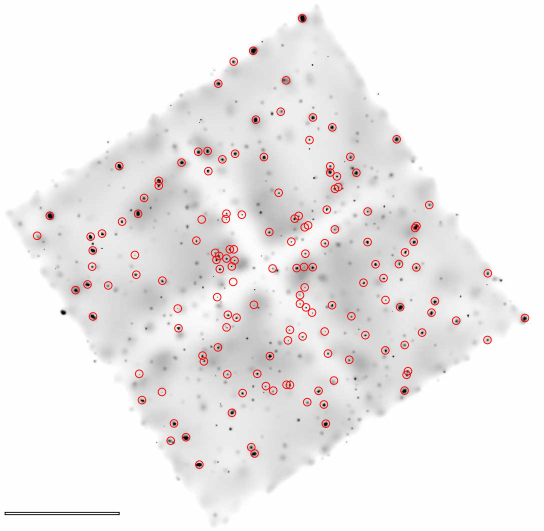

Fig. 2.— *Chandra* ACIS-I image of NGC 2516, smoothed like Fig. 1 and oriented in the same way and at the same scale (5 arcmin bar at lower left), but with the image center offset by $\sim 3.7'$ (cf. §2.1). Circles indicate ACIS-I detections.

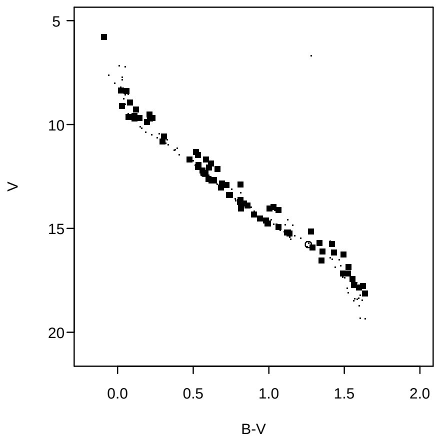

Fig. 3.— HR diagram of photometrically determined NGC 2516 cluster members. Squares indicate ACIS-I detections; a circle, an HRC-only detection within the ACIS-I FOV (a second such detection, at B-V=0.57,V=12.35, is not discernible at the resolution of this figure). Stars for which we derived only upper limits are denoted with small dots.

bands around fiducial main sequences in HR diagrams of both V–(B-V) and V–(V-I). In the V–(B-V) diagram, following a procedure described by Thurston (2000), we selected as possible members those stars in a band 0.9 magnitudes above and 0.3 below the fiducial main sequence of Pinsonneault et al. (1998) for [Fe/H]=-0.32. For the low mass domain we used the ZAMS model of Schmidt-Kaler (1982), smoothly connecting the curves by hand (cf. Thurston 2000). In the V–(V-I) diagram we selected stars in the same magnitude band about a main sequence derived from the theoretical models of D'Antona & Mazzitelli (1997) (cf. Thurston 2000 for a discussion of such an approach). Our final list combines those stars fulfilling both of the above criteria, when all three colors were available, and the V–(V-I) criterion alone, for the reddest stars having no B-V measurement. In summary we have 198 likely photometric members out of 1559 stars with known photometry and falling in the ACIS-I field of view. Table 2 gives the number of selected members observed (and detected) grouped according to spectral types (B, A, F, G , K, and M) photometrically assigned on the basis of reddening-corrected color-color ranges. Identifications have been performed

Table 3: Median log(L_X) for different spectral types, compared with values obtained for the Pleiades (Micela et al. 1999) cluster. Values in parenthesis denote upper limits.

Spectral type	color-color range	NGC 2516	Pleiades
B	$(B-V)_\circ < 0$	(28.81)	...
A	$0 < (B-V)_\circ < 0.3$	(28.91)	...
F	$0.3 < (B-V)_\circ < 0.5$	29.48	29.20
G	$0.5 < (B-V)_\circ < 0.8$	29.09	29.25
K	$0.93 < (V-I)_\circ < 2.2$	(28.98)	29.21
M	$2.2 < (V-I)_\circ < 3.0$	(28.85)	28.85

through positional matching with a match radius of 3″. The table shows that ∼42% of surveyed cluster members have been detected.

3. Results

3.1. X-ray Luminosity Functions

Computed *Chandra* X-ray luminosity functions are shown in Fig. 4 for three groupings of spectral types (B, A and F, G and K, and M alone), chosen to accentuate putative differences between NGC 2516 and the similarly young Pleiades. In the first and last cases, this comparison finds the two clusters indistinguishable. In the intermediate case shown in Fig. 4b, there is a suggestion (at the 95% confidence level) of a possible difference. Table 3, which compares the median log(L_X) values of these same two relatively young clusters, indicates that X-ray luminosities are highest for F and G stars. B- and A-type stars are problematic, not only due to incompleteness of our survey but also because of the issue of unresolved companions.

3.2. Estimate of X-ray field object contamination

In order to understand the level of contamination from field objects, we have computed the expected numbers of such unrelated objects, using the log N − log S relations of both Hasinger et al. (1993) and Branduardi-Raymont et al. (1994) and taking PIMMS conversion factors from models with power-law photon indexes in the range -1

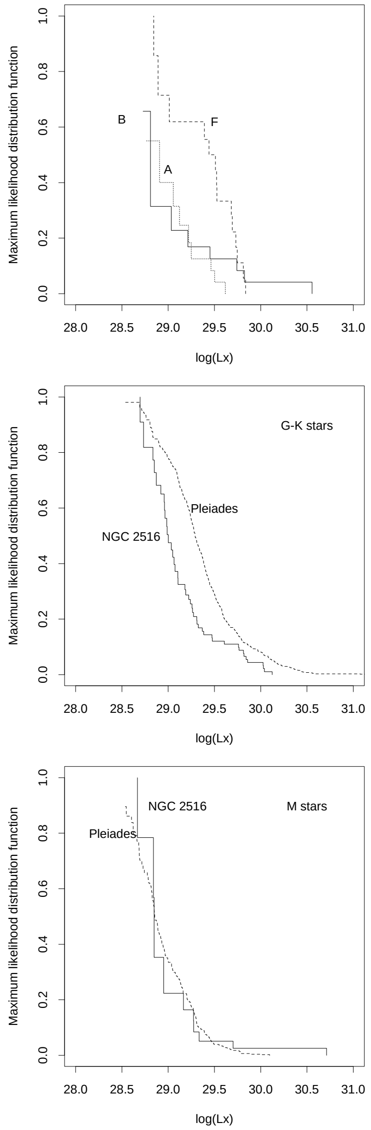

Fig. 4.— [(a) top-panel]: *Chandra* 0.1–4 keV X-ray luminosity functions for NGC 2516 cluster members of spectral types B , A and F as labeled. [(b) center-panel]: *Chandra* 0.1–4 keV X-ray luminosity function for cluster members of spectral types G and K. Dashed line indicates the analogous function for the Pleiades cluster measured with ROSAT. The two distributions differ at the 95% confidence level. [(c) bottom-panel]: Same as Fig. 4b, but for cluster members of spectral type M which is indistinguishable from that of their Pleiades cluster counterparts.

to -2 for fluxes in the 0.5 to 2.0 keV band from which the relations were derived, and with an integrated column density toward NGC 2516 of $N_H = 1.2\times10^{21}$ cm^{-2} (i.e., the total column out of the Galaxy as estimated from radio data with the *Chandra* proposal tool "colden"). These predictions are based on sensitivity maps derived from the *pwdetect* detection algorithm, using the actual acceptance thresholds for the HRC and ACIS, respectively[7]. The calculations show that, notwithstanding the smaller ACIS field of view (FOV), the number of X-ray sources associated with field objects is dominated by ACIS detections (though the HRC FOV is wider, the contribution from the outer portion of its field is less important due the effects on sensitivity of vignetting and the mirror's larger point spread function at large off-axis angles). We find that our survey is likely to contain between 19 and 31 field objects unrelated to NGC 2516.

As a further check we have computed the expected number of X-ray detections due to stars in the Galaxy with the XCOUNT model (Favata et al. 1992), obtaining a small contribution of about 3 detections. These are likely to be already included in number found in the above Log N - Log S calculation.

Since there are 74 (156-82) detections not associated with known cluster members, a large excess remains with respect to the predicted number of X-ray field sources computed above; the nature of this excess is unclear. Many of the objects responsible are likely to be of extragalactic nature, a suggestion reinforced by the fact that we have not found counterparts for 35 of our detections, very likely because they are below the photometric limit (V $\sim$ 20) of our catalogue. Ten or so of the remaining 39 sources are identified with stars above the NGC 2516 main sequence, implying that they are at smaller distances than NGC 2516 and could therefore be members of the Gould Belt (Guillout et al. 1998). Five others are identified with faint (V $\geq$ 16) blue objects and are likely of extragalactic nature. Due to the "fuzzy" main-sequence definition at faint magnitudes, a fraction of the sources identified with red stars could be faint cluster members.

[7]For more than half of the ACIS survey area we reach a limiting sensitivity of better than 10^{-14} erg sec^{-1} cm^{-2}, i.e., log (L_X)$\sim$ 29.25.

4. Discussion and Conclusions

NGC 2516 was chosen as a calibration target in order to "bore sight" the alignment of the X-ray telescope with the *Chandra* HRC-I and ACIS-I detectors. This cluster is of particular interest since, having a metallicity below solar, it allows us to explore the effect of metallicity on coronal emission level. Using ACIS hardness ratios to refine the derivation of X-ray fluxes, we have produced improved luminosity functions. Together with better photometry soon to be published (Jeffries, Thurston and Hambly, in preparation), even the present short *Chandra* calibration observations have enabled us to probe deeper into the population of cluster members and, for the first time, explore the X-ray emission of member stars redder than B-V > 1 (types K and later).

G and K stars in NGC 2516 tend to be less luminous than the G and K Pleiades stars, and NGC 2516 dM members are indistinguishable from their Pleiades counterparts, confirming the ROSAT HRI-based suggestion of Micela et al. (2000) that the activity level for dM stars is insensitive to a change of a factor of two in stellar metallicity. On the other hand, we find that the median log (L_X) value for NGC 2516 F-type stars is higher than that of the Pleiades, a firm result regardless of (any minimal) contamination from low L_X members.

The lack of astrometric proper motion studies and extensive radial velocity surveys of NGC 2516 stars has forced us to base our study on photometrically selected members. Such membership selection is subject to contamination from field stars that fortuitously have the same magnitude and colors as true NGC 2516 members. We have investigated the impact of this unavoidable contamination by examining available photometry for all objects in the ACIS-I FOV. From a quick analysis of the observed magnitude distribution in a few selected bins of B-V color, we have derived the contamination of field stars estimating their contribution to the observed number of stars in the magnitude strips populated by NGC 2516 members.

We estimate that non-member contamination could be up to 30% for the G and K stars, and up to 45% for later-type stars. This contaminating population is likely to be dominated by stars with X-ray luminosities lower than those of young NGC 2516 members; hence we expect them to go undetected in our X-ray survey (i.e., they should dominate the sample of stars for which we have derived only X-ray upper-limits), with their unavoidable inclusion contributing to a substantial lowering of the derived luminosity function with respect to the "true" one. If we were to assume that *all* stars for which we have no X-ray detections are *not* cluster members, then such contamination could explain the differences suggested above between the G- and K-star X-ray luminosity function of NGC 2516 as compared to that of the Pleiades. This extreme case would have little effect, however, on the results for M stars.

In order to be able to draw firm conclusions regarding metallicity effects on coronal emission it is crucial that an improved list of members be obtained. Available photometric data must be complemented with proper motion studies and with an extensive campaign of radial velocity measurements through high resolution spectroscopy.

Acknowledgments

The successful construction and operation of *Chandra*, a NASA "Great Observatory," is a stupendous undertaking requiring the dedication of a massive team. While we obviously cannot thank everyone individually, we do want to recognize the seminal efforts of H. Tananbaum, Director of the *Chandra* Observatory X-ray Center, and the key contributions of telescope scientist L. S. Van Speybroeck and instrument PIs S. S. Murray (HRC) and G. Garmire (ACIS). The work at CfA was partially supported by NASA contract NAS8-39073 and NASA grant NAS5-4967. F.D., E.F., G.M., N.P. and S.S. wish to acknowledge support from Italian Space Agency (ASI) and MURST. RDJ acknowledges the support of the Leverhulme Trust.

References

Branduardi-Raymont, G., Mason, K. O., Warwick, R. S. et al. 1994, MNRAS, 270, 947

Cox, A.N. 1995, ApJ, 121, 628

Damiani, F., Maggio, A., Micela, G., Sciortino, S. 1997a, ApJ, 483, 350

Damiani, F., Maggio, A., Micela, G., Sciortino, S. 1997b, ApJ, 483, 370

D'Antona, F., & Mazzitelli I. 1997, MemSAIT, 68, 807

Favata F., Micela G., Sciortino S., Vaiana, G. S. 1992, A&A, 256, 86

Guillout, P., Sterzik, M.F., Schmitt, J.H.M.M., Motch, C., Neuhaeuser, R., 1998, A&A, 337, 113

Hasinger, G., Burg, R., Giacconi, R. et al. 1993, A&A, 275, 1

Jeffries, R. D., Thurston, M. R., and Pye, J. P. 1997, MNRAS, 287, 350 [JTF97]

Micela, G., Sciortino, S., Harnden, F. R., Jr. et al. 1999, A&A, 341, 751

Micela, G., Sciortino, S., Jeffries, R.D., Thurston, M.R. & Favata, F. 2000, A&A, 357, 909

Kenter, A., Chappell, J.H., Kraft, R., Meehan, G., Murray, S.S., Zombeck, M., Hole, K.T., Juda, M., Donnelly, R.H., Patnaude, D., Pease, D., Wilton, C., Zhao, P., Austin, G., Fraser, G., Pearson, J., Lees, J., Brunton, A., Barbera, M., Collura, A., & Serio, S. 2000, SPIE, in press

Murray, S. S., Austin, G., Chappell, J. H., Gomes, J., Kenter, A., Kraft, R., Meehan, G., Zombeck, M., Fraser, G., Serio, S. 2000, SPIE, 4012, 68

Pinsonneault et al. 1998, ApJ, 504, 170

Schmidt-Kaler, Th. 1982 in K.H. Hellwege ed., Landolt-Börnstein New Series, Volume VI/2b, Springer-Verlag, Berlin, Heidelberg, p.1

Townsley, L. K., Broos, P. S., Garmire, G. P., Nousek, J. A. 2000, ApJ Letters, 534, L139

Thurston, M. R. 2000, Ph. D. Thesis, Keele University